

# Hybrid Plasmonic Whispering-gallery-mode Ring Resonator at NanoScales

Feifei Shi, Xin Gong, Zhaoyu Zhang\*  
 School of Electronic and Computer Engineering,  
 Peking University Shenzhen Graduate School  
 Shenzhen, China

\*corresponding author: zhangzy@pkusz.edu.cn

**Abstract**—a hybrid plasmonic whispering-gallery-mode cavity comprising of a semiconductor ring separated from a metal surface by a nanoscale dielectric gap is proposed and numerically investigated. The nanoscale ring resonator supports hybrid plasmonic modes with highly localized electromagnetic fields, featuring an ultra-small mode volume  $\sim 0.00129 \text{ um}^3$ . The total quality factor is found to be limited by two mechanisms, the metal radiation loss and the absorption loss, and exhibits a tradeoff with the mode volume.

**Keywords**—whispering-gallery-mode; surface plasmon; ring resonator;

## I. INTRODUCTION

Light confinements in wavelength-scale nanocavities have been attracting considerable attention, owing to their ability to strongly enhance light-matter interactions. Strong interactions enable nanocavities as one of key components for novel photonic devices such as efficient single photon sources [1] and optical switches [2]. In particular, plasmonic cavities are attractive because they can support resonant modes with subwavelength mode volumes in contrast to dielectric cavities [3,4]. On the other hand, among dielectric cavities, whispering-gallery-modes (WGM) excited at disk or ring cavities have been studied over a wide range of applications such as memories [5] and lasers [6]. However, conventional WGM dielectric cavities suffers the limitation of size reduction. Very recently, many researchers have reported the plasmonic WGM cavities based on surface plasmon polaritons (SPPs), which are electron density waves excited at the interfaces between metals and dielectric materials. The plasmonic WGM cavities, which support WGM in subwavelength size, reveal as potential a new building blocks for the high-density integration of photonic devices due to its small size.

In this letter, we propose a deep-subwavelength-sized hybrid plasmonic WGM nanocavity comprising of a semiconductor ring separated from a metal surface by a nanoscale dielectric gap. The ring radius is varied from 200 nm to 500 nm to achieved optimal performance. The cavity mode shows an ultra-small mode volume of  $0.0066(\lambda_0)^3$  ( $\lambda_0$ : free space wavelength of around 580 nm). In addition, we divide hybrid plasmonic resonator loss into radiation loss and metallic

absorption loss. The total quality factor is found to be limited by these two factors and exhibits a tradeoff with the mode volume.

## II. GEOMETRY AND MODAL PROPERTIES OF THE PROPOSED HYBRID RIGN RESONATOR

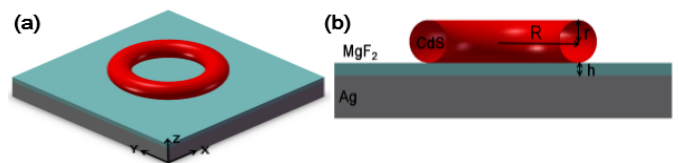


Fig. 1. (a) Schematic of the hybrid plasmonic WGM nanocavity. (b) Cross-sectional view of the hybrid plasmonic WGM nanocavity consisting of a cadmium sulphide (CdS) ring atop a silver surface separated by a 5-nm-thick magnesium fluoride ( $\text{MgF}_2$ ) gap layer. The refraction indices of the media are  $n_{\text{CdS}} = 2.5$  and  $n_{\text{MgF}_2} = 1.4$ , respectively; the permittivity data of silver is from Johnson and Christy data. The ring has a variable radius  $R$  and fixed cross-section radius  $r$  of 60 nm.

Fig. 1(a) shows a schematic diagram of the hybrid plasmonic nanocavity consisting of a cadmium sulphide (CdS) ring atop a silver surface separated by a 5-nm-thick magnesium fluoride ( $\text{MgF}_2$ ) gap layer. The refractive indices of the ring and the gap dielectric are  $n_{\text{CdS}} = 2.5$  and  $n_{\text{MgF}_2} = 1.4$ , respectively. We choose to use silver, a relatively low loss metal in the visible spectrum, whose permittivity data is from Johnson and Christy[7]. The ring has a radius of  $R$  and its cross-section radius  $r$  is fixed at 60 nm. The modal properties are investigated by means of finite difference time domain method (FDTD). Perfectly matched layers (PML) boundary conditions are employed to absorb incident light with zero reflection. The simulations will end when the total energy in the simulation volume drops to  $10^{-5}$  of the maximum energy injected.

Fig. 2(a) shows that the light is tightly confined and the field is greatly enhanced in the gap layer. We can understand this enhancement by the index discontinuity at the CdS and  $\text{MgF}_2$  interface which generates polarization charges interacting with the plasmon oscillations at the metal- $\text{MgF}_2$  interface. The electric field ( $E_z$ ) profiles of the hybrid modes are shown in Fig. 2(b)-(d) with resonance wavelengths around 580nm and different azimuthal numbers  $m = 5$ ,  $m = 7$  and  $m = 10$  for ring resonators with different radii 250 nm, 350 nm and 500 nm, respectively. We consider a cavity with more localized modes designed for a specific resonant wavelength of 580 nm.

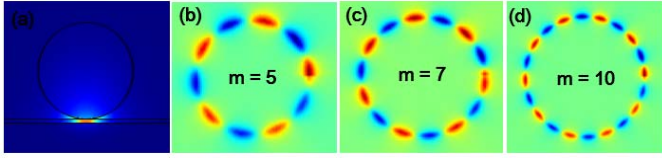


Fig. 2. (a) Cross-sectional view of the electric field energy intensity; (b)-(d) Horizontal view of the electric field ( $E_z$ ) of the plasmonic WGM mode with resonant wavelength around 580nm in the visible spectrum and different azimuthal numbers  $m = 5$ ,  $m = 7$ , and  $m = 10$  with relevant radii of 250 nm, 350 nm and 500 nm, respectively.

In order to achieve deep subwavelength cavity size with the resonant wavelength around 580 nm while maintaining favorable resonance performance, the resonant wavelength, Q factor, and mode volume were systematically investigated in Fig. 2 by varying the plasmonic ring radius (or azimuthal number). The resonance wavelength increases with increasing radius seen from Fig. 2(a). The quality factor  $Q$  is defined as  $Q = \omega_0(\text{Stored Energy})/(\text{Power Loss})$ , and calculated from the time decay of the cavity energy. The total Q factor (Q-total) decreases with decreasing radius, shown in Fig. 2(b). Total loss of the hybrid plasmonic cavity can be divided into optical loss by radiation and metallic loss by absorption. In order to systematically investigate the dependence of Q factor on the radius, Q-optical and Q-absorption were calculated separately, where Q-optical was estimated by setting the imaginary part of permittivity of silver to zero. Here, Q-optical and Q-absorption are inversely proportional to the optical loss and absorption

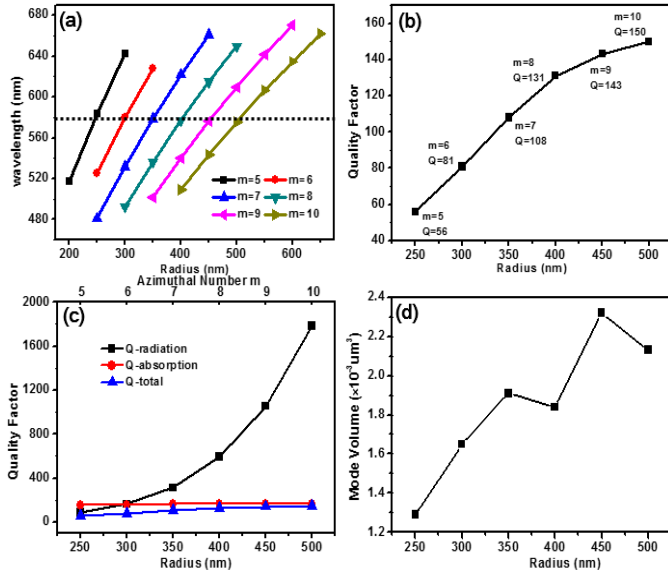


Fig. 2. (a) Resonant modes for various ring radius, the dotted black line indicates resonant wavelength  $\lambda_0 = 580$  nm; (b) The total Q factor versus ring radius; (c) Q factors of hybrid plasmonic WGM for various ring radii. The top axis shows the corresponding azimuthal numbers to the radii of the cavities, and the modes have almost the same resonant wavelength of 580 nm: mode with  $R = 250$  nm gives  $m = 5$  with  $\lambda_0 = 583$  nm and  $Q = 56$ , mode with  $R = 300$  nm gives  $m = 6$  with  $\lambda_0 = 580$  nm and  $Q = 81$ ,  $R = 350$  nm gives  $m = 7$  with  $\lambda_0 = 579$  nm and  $Q = 108$ , mode with  $R = 400$  nm gives  $m = 8$  with  $\lambda_0 = 577$  nm and  $Q = 131$ , mode with  $R = 450$  nm gives  $m = 9$  with  $\lambda_0 = 576$  nm and  $Q = 143$ , and mode with  $R = 500$  nm gives  $m = 10$  with  $\lambda_0 = 575$  nm and  $Q = 150$ . Q-total, Q-optical, and Q-absorption are indicated by blue, black, and red lines, respectively; (d) Mode volume versus ring's radius.

loss, respectively. Interestingly, when radius is larger than 350 nm, Q-total is dominated by Q-absorption and, when radius is smaller than 250 nm, Q-total is dominated by Q-optical. Q-optical exponentially decreases with a decreasing radius, which can be understood by larger radiation loss due to the smaller radius of the curvature.

The mode volume is one of the key parameters for a resonator, which is defined as the ratio of the total energy density of the mode to the peak energy density. From Fig. 2(d) Mode volume shows a rising tendency with increasing the ring's radius, which is due to less strong confinement of light at bigger radius. The mode volume changes from  $0.0066 \lambda_0^3 \sim 1.29 \times 10^{-3} \text{ um}^3$  to  $0.012 \lambda_0^3 \sim 2.32 \times 10^{-3} \text{ um}^3$ , where  $\lambda_0$  is the free space wavelength of 580 nm. Therefore, we get a hybrid plasmonic nanocavity with an ultra-small mode volume.

### III. CONCLUSION

The hybrid plasmonic whispering-gallery-mode nanocavity, which comprises of a semiconductor ring above a metal surface separated by a nanoscale dielectric gap, is introduced and its performance is analyzed. Hybrid plasmonic modes with highly localized electromagnetic fields are found in the nanoscale resonator. The cavity mode has an ultra-small mode volume  $0.0066(\lambda_0)^3$  ( $\lambda_0$ : free space wavelength of around 580 nm). The total quality factor is limited by the metal absorption loss and the radiation loss, and exhibits a tradeoff with the mode volume.

### ACKNOWLEDGMENT

This work is supported by Startup Fund by the Peking University Shenzhen Graduate School. The authors are grateful for the valuable discussions with Chuanhong Liu in the same group.

### REFERENCES

- [1] J. Reithmaier, G. Sęk, A. Löffler, C. Hofmann, S. Kuhn, S. Reitzenstein, et al., "Strong coupling in a single quantum dot-semiconductor microcavity system," *Nature*, vol. 432, pp. 197-200, 2004.
- [2] K. Nozaki, T. Tanabe, A. Shinya, S. Matsuo, T. Sato, H. Taniyama, et al., "Sub-femtojoule all-optical switching using a photonic-crystal nanocavity," *Nature Photonics*, vol. 4, pp. 477-483, 2010.
- [3] B. Min, E. Ostby, V. Sorger, E. Ulin-Avila, L. Yang, X. Zhang, et al., "High-Q surface-plasmon-polariton whispering-gallery microcavity," *Nature*, vol. 457, pp. 455-458, 2009.
- [4] R. F. Oulton, V. J. Sorger, T. Zentgraf, R.-M. Ma, C. Gladden, L. Dai, et al., "Plasmon lasers at deep subwavelength scale," *Nature*, vol. 461, pp. 629-632, 2009.
- [5] M. T. Hill, H. J. Dorren, T. De Vries, X. J. Leijtens, J. H. Den Besten, B. Smalbrugge, et al., "A fast low-power optical memory based on coupled micro-ring lasers," *nature*, vol. 432, pp. 206-209, 2004.
- [6] M. Fujita, A. Sakai, and T. Baba, "Ultrasmall and ultralow threshold GaInAsP-InP microdisk injection lasers: design, fabrication, lasing characteristics, and spontaneous emission factor," *Selected Topics in Quantum Electronics, IEEE Journal of*, vol. 5, pp. 673-681, 1999.
- [7] P. B. Johnson and R.-W. Christy, "Optical constants of the noble metals," *Physical Review B*, vol. 6, p. 4370, 1972.